Free Radical Biology and Medicine 108 (2017) 174–182

Contents lists available at ScienceDirect

Free Radical Biology and Medicine

journal homepage: www.elsevier.com/locate/freeradbiomed

Selenoprotein T is required for pathogenic bacteria avoidance in *Caenorhabditis elegans*

Laura Romanelli-Cedrez[a,b], Inés Carrera[a], Lucía Otero[a], Antonio Miranda-Vizuete[c], Marco Mariotti[d], Mark J. Alkema[e], Gustavo Salinas[a,b,*]

[a] *Worm Biology Laboratory, Institut Pasteur de Montevideo, Uruguay*
[b] *Cátedra de Inmunología, Departamento de Biociencias, Facultad de Química, Universidad de la República, Montevideo, Uruguay*
[c] *Instituto de Biomedicina de Sevilla (IBIS), Hospital Universitario Virgen del Rocío/CS IC/Universidad de Sevilla, 41013 Sevilla, Spain*
[d] *Division of Genetics, Department of Medicine, Brigham and Women's Hospital and Harvard Medical School, Boston, MA, United States of America*
[e] *C. elegans Behavorial Genetics Laboratory, Neuroscience Department, University of Massachusetts Medical School, Worcester, MA, United States of America*

ARTICLE INFO

Keywords:
C. elegans
Nematode
Selenocysteine
Selenoprotein T
SelT
SelenoT
Serratia marcescens
Pseudomonas aeruginosa
Pathogenic bacteria avoidance

ABSTRACT

Selenoprotein T (SELENOT) is an endoplasmatic reticulum (ER)-associated redoxin that contains the amino acid selenocysteine (Sec, U) within a CXXU motif within a thioredoxin-like fold. Its precise function in multicellular organisms is not completely understood although it has been shown in mammals to be involved in Ca^{2+} homeostasis, antioxidant and neuroendocrine functions. Here, we use the model organism *C. elegans* to address SELENOT function in a whole organism throughout its life cycle. *C. elegans* possess two genes encoding SELENOT protein orthologues (SELT-1.1 and SELT-1.2), which lack Sec and contain the CXXC redox motif instead. Our results show that a Sec→Cys replacement and a gene duplication were two major evolutionary events that occurred in the nematode lineage. We find that worm SELT-1.1 localizes to the ER and is expressed in different cell types, including the nervous system. In contrast, SELT-1.2 exclusively localizes in the cytoplasm of the AWB neurons. We find that *selt-1.1* and *selt-1.2* single mutants as well as the double mutant are viable, but the *selt-1.1* mutant is compromised under rotenone-induced oxidative stress. We demonstrate that *selt-1.1,* but not *selt-1.2*, is required for avoidance to the bacterial pathogens *Serratia marcescens* and *Pseudomonas aeruginosa*. Aversion to the noxious signal 2-nonanone is also significantly impaired in *selt-1.1*, but not in *selt-1.2* mutant animals. Our results suggest that *selt-1.1* would be a redox transducer required for nociception and optimal organismal fitness. The results highlight *C. elegans* as a valuable model organism to study SELENOT-dependent processes.

1. Introduction

Selenium (Se) is an essential trace element in many organisms, including humans and its deficiency in mammals is a contributing factor to various pathologies and disorders (reviewed in [1]). Se supports several cellular and organismal processes including development [2,3], immunity [4], reproduction [5], neuromuscular [2]. Se is required for the function of selenoproteins, which contain the 21st amino acid selenocysteine (Sec, three letter code or U, one letter code) as a catalytic redox-active residue [1,6,7]. Sec is a Se-containing analogue of Cys, where the selenol group of Sec fulfills the same redox role as the thiol group of Cys, but usually confers a catalytic advantage over thiol [8]. Sec is encoded by an in frame UGA codon and a SElenoCysteine Insertion Sequence (SECIS) present in the 3´-untranslated region (3´-UTR) of selenoprotein mRNAs, and decoded by a $tRNA^{Sec}$, a dedicated elongation factor (EfSec), and a SECIS-binding protein (SBP2) [9,10]. Selenoproteins of known functions serve as oxidoreductases. However, the function of several selenoproteins remains unknown or poorly understood.

Selenoproteins T, V, W, and H (SELENOT, SELENOV, SELENOW and SELENOH) and Rdx12 belong to the redoxin family of selenoproteins, and their precise functions remain elusive. Redoxins are presumed thiol/selenol-based oxidoreductases that possess a domain that belongs to the thioredoxin (Trx) folding unit with a CXXU or CXXC redox motif and a conserved C-terminal TGXFEI consensus motif that is considered the gene signature of the redoxin family [11].

Abbreviations: ER, endoplasmic reticulum; NGM, nematode growth medium; Se, selenium; Sec, selenocysteine; SELENOT, selenoprotein T; SELT-1.1, selenoprotein T1; SELT-1.2, selenoprotein T2; Trx, thioredoxin. Note: the use of the root symbol SELENO followed by a letter has been recently accepted for vertebrate selenoprotein gene nomenclature. *C. elegans* gene nomenclature is restricted to a maximum of four letters and thus we used the previous root, selt, when referring to *C. elegans* genes

* Corresponding author at: Worm Biology Laboratory, Institut Pasteur de Montevideo, Uruguay, Mataojo 2020, CP-11400 Montevideo, Uruguay.
E-mail address: gsalin@fq.edu.uy (G. Salinas).

http://dx.doi.org/10.1016/j.freeradbiomed.2017.03.021
Received 16 October 2016; Received in revised form 15 March 2017; Accepted 20 March 2017
Available online 24 March 2017
0891-5849/

SELENOT has a discontinuous Trx domain, which is interrupted by transmembrane helices, that are presumed to anchor this protein to the endoplasmic reticulum membrane (ER) [11,12]. In mammals, *SELENOT* is an essential gene [13] and it has been implicated in the regulation of Ca^{2+} homeostasis, antioxidant and neuroendocrine functions [12,13]. *SELENOT* was identified as a gene that is regulated by the neuropeptide pituitary adenylate cyclase-activating polypeptide (PACAP). Overexpression of wild-type *SELENOT*, but not a Sec→Ala mutant, in the catecholaminergic cell line PC12 resulted in an increase of the intracellular Ca^{2+} levels and growth hormone secretion [12]. SELENOT has been found to be expressed in mouse and human pancreatic β-cells and its targeted inactivation impairs glucose tolerance in conditional β-cells *SELENOT* knockout (KO) mice [14]. Recently, the conditional KO mice were shown to be more sensitive to Parkinson disease-inducing neurotoxins, leading to motor impairment associated with oxidative stress and decreased tyrosine hydroxylase activity and dopamine synthesis [13]. These results suggest that SELENOT plays a role in the protection of dopaminergic neurons under stress conditions. Other experiments have shown that knockdown of *SELENOT* in mouse fibroblasts led to overexpression of other oxidoreductases, including the redoxin SELENOW, and altered expression of extracellular matrix genes and cell adhesion [15]. Yet, despite these advances, the function of SELENOT remains unknown.

In contrast with the relative high number of redoxins in mammals (SELENOT, SELENOV, SELENOW, SELENOH, and Rdx12), the *Caenorhabditis elegans* genome encodes only two redoxins, both belonging to the SELENOT subfamily, SELT-1.1 and SELT-1.2 [16]. Furthermore, *C. elegans* SELT-1.1 and SELT-1.2 contain Cys at the Sec homologous position in mammalian SELENOT.[1] Despite the lack of Sec, the selenoprotein T name is retained in *C. elegans*, and to follow *C. elegans* nomenclature, we will use SELT as name. This makes *C. elegans* a particularly suited organism to address the function of SELENOT proteins, since close homologs in which Sec is replaced by Cys do not seem to affect the protein function of selenoproteins [17,18]. In this work we show that the Sec to Cys replacement and gene duplication of SELENOT were two major evolutionary events in nematodes. We found that *C. elegans selt-1.1* and *selt-1.2* single mutant as well as the double mutant are viable. A detailed phenotypic analysis of *selt-1.1* and *selt-1.2* mutant strains revealed that SELT-1.1, but not SELT-1.2, have defects in nociception. Importantly, SELT-1.1 is required for pathogenic bacteria avoidance. Our results highlight *C. elegans* as the first animal in which SELENOT function can be addressed at the organismal level.

2. Material and methods

2.1. Strains and culture conditions

The wild-type strain used in this study was *C. elegans* Bristol N2 (N2), which was grown monoxenically in the *Escherichia coli* strain OP50 as a food source. N2 and OP50 were obtained from the *Caenorhabditis* Genetic Center (CGC). The general methods used for culturing and maintenance of *C. elegans* are described in [19].

The *selt-1.1*(*tm3763*) *X* and *selt-1.2*(*tm3771*) *V* deletion mutant strains were obtained from the *C. elegans* National Bioresource Project of Japan. A scheme depicting the deletions harbored by these strains is shown in Fig. 1. The deletion mutant strains were outcrossed 6-times with the N2 strain. All strains generated and used in this study are detailed in **Supplementary Table 1**.

Transgenic lines were obtained according to [20]. The pL15EK plasmid containing the injection marker *lin-15* (80 ng/μL) was co-injected with constructs containing either *Pselt-1.1*::*gfp*, *Pselt-1.2*::*gfp*, *Pselt-1.1*::*selt-1.1*::*gfp* or *Pselt-1.2*::*selt-1.2*::*gfp* cloned into the pPD95.77 plasmid and injected into *lin-15(n765ts)* animals. For each construct at least three independent transgenic lines were isolated and observed. The integrated transgenic QW1265 and QW1266 strains were obtained by X-ray irradiation.

The *E. coli* strain HT115 containing the empty pL4440 plasmid and the pL4440 derivative containing the ER thiol-disulfide oxidoreductases and *dpy-11* were kindly provided by Dr. Peter Askjaer (detailed in **Supplementary Table 2**).

2.2. Green Fluorescent Protein reporter constructs for expression and localization analysis

Four constructs using the Green Fluorescent Protein (GFP) as a reporter were generated to determine *selt-1.1* and *selt-1.2* expression patterns. The transcriptional *Pselt-1.1*::*gfp* and *Pselt-1.2*::*gfp* fusions correspond to *selt-1.1* and *selt-1.2* promoters upstream of the *gfp* coding sequence. The promoter sequences comprise the upstream sequence of coding sequence up to the beginning of the adjacent gene (2 kbp and 0.6 kbp for *selt-1.1* and *selt-1.2*, respectively) (Fig. 1). Sequences were amplified by PCR using appropriate primers including *Sal*I and *Bam*HI restriction sites for *Pselt-1.1,* and *Sal*I and *Hin*dIII for *Pselt-1.2* (**Supplementary Table 3**). Genomic DNA from adult worms of the N2 strain was used as a template. The PCR products were cloned into the pPD95.77 vector. Translational constructs *Pselt-1.1*::*selt-1.1*::*gfp* and *Pselt-1.2*::*selt-1.2*::*gfp* include promoter, exons and introns of the gene of interest (Fig. 1) in frame with the *gfp* coding sequence. The *unc-54* 3'UTR sequence provided by the vector was used in both, transcriptional and translational constructs. The restriction sites used for cloning and the vector were the same as for the transcriptional constructs fusions. A scheme depicting the sequence of *Pselt-1.1*::*gfp*, *Pselt-1.2*::*gfp*, *Pselt-1.1*::*selt-1.1*::*gfp* and *Pselt-1.2*::*selt-1.2*::*gfp* used for the transcriptional and translational reporter constructs is shown in Fig. 1.

2.3. DiI staining

Animals were incubated in 1 mL M9 buffer (KH_2PO_4 3 g/L, Na_2HPO_4 6 g/L, NaCl 5 g/L, $MgSO_4$ 1 mM) solution with 0.6 μg/mL of the compound DiI (1,1'-Dioctadecyl-3,3,3',3'-Tetramethylindocarbocyanine Perchlorate, $C_{59}H_{97}ClN_2O_4$) for 30 min with gentle shaking at room temperature. Then, worms were washed four times with M9, centrifuging at 600 g for 1 min, each time removing the supernatant and adding 1 mL of M9 again. After washing the worms were placed on a NGM-agar plate with food, allowed to recover overnight at 20 °C and imaged next day.

2.4. Fluorescence microscopy

Worms were mounted in a drop of 60 mM sodium azide, over a thin layer of 2% agarose. Individual animals were visualized under a microscope TCS SP5 Leica DMI6000 and images captured with Lasaf 2.7 software and processed with Fiji [21]. Embryos were visualized under a microscope Olympus IX81 with a camera Hamamatsu ORCA ER and images were captured with 4.17 micro-manager software [22]. The images were processed using FIJI and Huygens 4.5.lp3 programs. Embryos were obtained by a transverse cut in a gravid adult (for the early stages) or picked directly from the plate (for late embryonic stages) and mounted on a slide with an agarose layer as described above.

2.5. RNA interference assay

The expression of all *C. elegans* ER thiol-disulfide oxidoreductases containing the canonical ER retaining sequences (KDEL or variants of this motif) [23] were interfered by RNAi (**Supplementary Table 2**).

[1] The use of the root symbol SELENO followed by a letter has been recently accepted for vertebrate selenoprotein gene nomenclature. *C. elegans* gene nomenclature is restricted to a maximum of four letters and thus we used the previous root, selt, when referring to *C. elegans* genes. *selt-1.1* and *selt-1.2* designation is suggested by the wormbase as they represent recent duplication in nematodes.

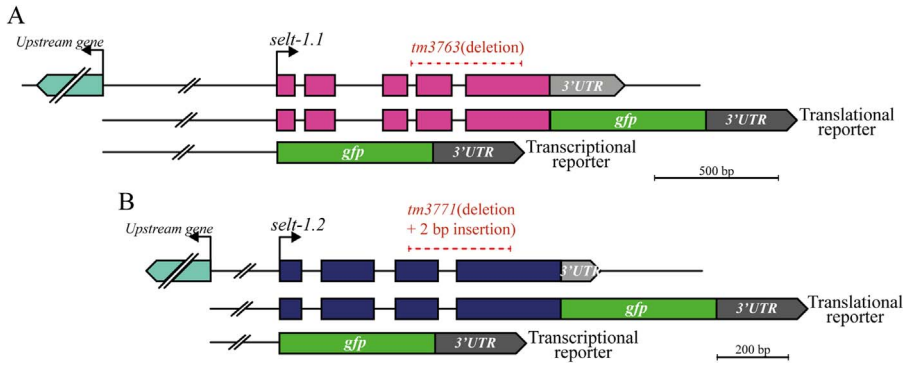

Fig. 1. *selt-1.1* (A) and *selt-1.2* (B) gene structure, deletion intervals and constructs generated for transgenic animals. Exons of the two genes are shown as pink (*selt-1.1*) and blue (*selt-1.2*) boxes connected by lines representing introns. *selt* 3'UTRs are shown as light grey boxes. The red dashed lines indicate the *selt-1.1(tm3763)* and *selt-1.2(tm3771)* deletion alleles. The *tm3763* mutation deletes 429 bases. The *tm3771* mutation deletes 275 bases and inserts 2 bases. A scheme of the translational and transcriptional constructs used for the generation of transgenic animals is shown below each gene. In both cases the 3'UTR used is the one from *unc-54* provided by the vector (pPD95.77) indicated by dark grey boxes. (For interpretation of the references to color in this figure legend, the reader is referred to the web version of this article).

The *E. coli* strain HT115 containing the plasmid pL4440 encoding the gene of interest were grown over night at 37 °C in LB (Luria-Bertani) with 100 μg/mL ampicillin. Plasmids without an insert DNA (empty) or encoding *dpy-11* were used as negative and positive controls, respectively. The bacteria were plated in agar NMG 100 μg/mL ampicillin and 1 mM IPTG (required for induction of double-stranded RNA expression) and incubated over night at 37 °C. Twenty adult worms of N2 and the *selt-1.1(tm3763); selt-1.2(tm3771)* double mutant strain were placed on plates for 1 h and then removed leaving only the eggs, the latter corresponding to the F0 generation. Phenotypes were monitored from the F1 to the F5 generation. The differences in locomotion, development, early death and modified morphology between strains were monitored.

2.6. Volatile chemotaxis assays

Avoidance assays with 2-nonanone was performed according to [24], with the following modification: well fed adult worms were washed 3 times with NMG buffer, centrifuged at 600*g* for 1 min, each time removing the supernatant and adding 1 mL of NMG buffer again. Chemotaxis assays with isoamyl alcohol and 1-octanol was performed according to [25].

2.7. Pathogenic bacteria lawn avoidance assay

Lawns of *Serratia marcescens* (50 μL of an overnight LB culture) were cultured on 6-cm NGM plates overnight at room temperature. Approximately 20 young adult animals grown on OP50 were put in the center of the bacteria lawn [26]. The number of animals on each lawn was counted after 20 h. *Pseudomonas aeruginosa* PA14 were grown overnight in LB culture without shaking. 30 μL overnight culture was seeded on 9-cm NMG plates and incubated for 24 h at room temperature. Approximately 30 well-fed L4-young adults were added on the assay plates. The number of animals remaining on the lawn after 24 h was counted [27].

2.8. Rotenone stress assays

Synchronized adults (~200) of N2 and *selt-1.1(tm3763)* strains were incubated 4 h with 50 μM of rotenone in M9 buffer at room temperature with gently shaking. After incubation, worms were washed two times with M9 centrifuged at 600*g* for 1 min, each time removing the supernatant and adding 1 mL of M9 again. Finally worms were transferred to 5 cm plates seeded with OP50 for 60 h and scored the number of alive and dead. In both cases vehicle control (DMSO 3%) were included. Experiments were repeated three times, each time including two replicates per condition per strain.

2.9. Nematode SELENOT gene identification and phylogeny

The two *C. elegans selt* genes were identified through blast searches using the human gene as query. We then extended the search to all publicly available nematode genomes. For this task, all nematode assemblies available at NCBI were downloaded and searched iteratively with Selenoprofiles [28] using a profile alignment of SELENOT proteins progressively enriched in nematode sequences. The phylogenetic tree of the predicted protein sequences was reconstructed by maximum likelihood using phyml 3.0 [29], with the evolutionary model resulting from an automated selection procedure (LG), as explained in [30]. The protein tree was compared with the known species phylogeny, obtained from NCBI taxonomy [31] and refined according to [32].

3. Results

3.1. A Sec to Cys replacement and a selt gene duplication occurred in the nematode lineage

Using blastX homology searches with the human SELENOT protein we identified two *selt* genes, *selt-1.1* (formerly C35C5.3) and *selt-1.2* (formerly F28H7.4) in the *C. elegans* genome. Both *selt-1.1* and *selt-1.2* genes encode proteins that possess an N-terminal putative CVSC redox motif and the C-terminal GAFEI/V motif within a thioredoxin folding unit, which are the gene signature of the redoxin family. The thioredoxin domain is interrupted by a hydrophobic region, which constitutes the gene signature of the redoxin SELENOT (**Supplementary Fig. 1**). The identified *C. elegans* protein sequences were then retroblasted towards mammalian genomes and the single hit obtained was SELENOT.

Next, we examined the nematode lineage for the presence of *selt* genes. The majority of species of class *Chromadorea* have a single copy of *selt*, with exceptions of most species in the *Rhabditoidea* superfamily (which includes *C. elegans*), *Meloidogyne incognita*, and *Rotylenchulus reniformis* (**Supplementary Fig. 2**). Most *Caenorhabditis* genomes analyzed possess two *selt* genes (*selt-1.1* and *selt-1.2*) and *C. brenneri* possess a third *selt* gene, and *C. japonica* possess only a single *selt* gene, orthologous to *C. elegans selt-1.1*(Fig. 2 **and Supplementary Fig. 2**)[32]. *Caenorhabditis* spp. *selt-1.2* differs from *selt-1.1* (45% identity, 57% similarity), suggesting diversification of function after gene duplication. The third *selt* gene present in *C. brenneri* is highly similar in sequence to *selt-1.2*, suggesting a recent duplication event or a sequencing/assembling artifact. A similar explanation would account for the presumed *selt* gene duplication events observed in *Meloidogyne incognita* and *Rotylenchulus reniformis*.

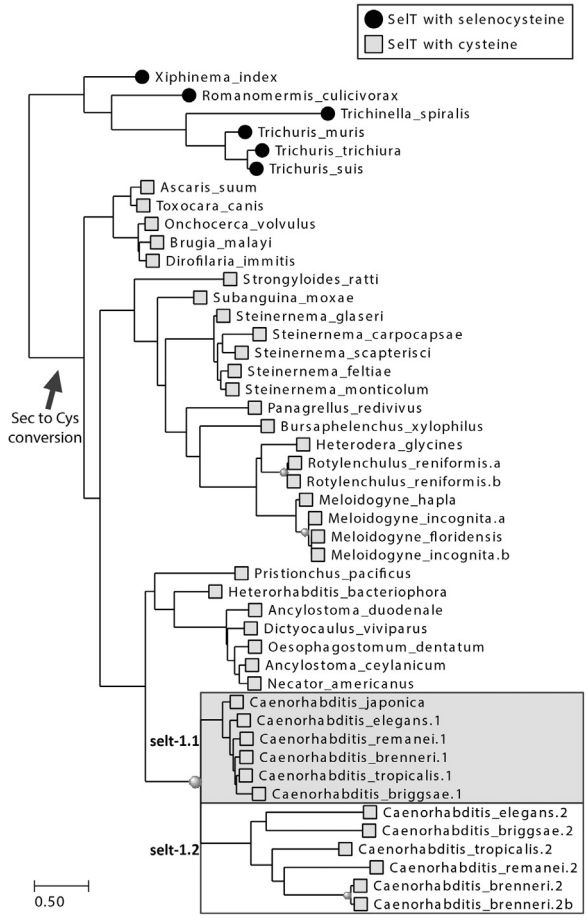

Fig. 2. Phylogenetic tree of nematode *SELENOT* genes. The Figure shows the phylogenetic tree of nematode *SELENOT* genes identified in this study, reconstructed based on their protein sequence. Black circles and grey rectangles are used to represent the Sec- and Cys-containing SELENOT, respectively. Grey circles on the internal nodes are used to indicate the predicted gene duplication events. The group of *Rhabditoidea selt-1.1* and *selt-1.2* proteins is highlighted in light grey and white boxes, respectively. The scale represents the distance between protein sequences, in average substitutions per site.

Most animals possess a Sec-containing SELENOT. However, we found that nematodes that belong to class *Chromadorea* encode Cys-containing SELENOT, whereas those of the *Enoplea* class (e.g. *Trichuris muris*, *Trichinella spiralis*) encode Sec-containing SELENOT. In these latter cases we found an in frame UGA codon and a selenocysteine insertion signal (SECIS) at the 3'-UTR of the mRNA, as expected for selenoproteins. *Enoplea* is considered to be the most ancestral nematode lineage (Fig. 2)[33].

Altogether, these observations support that there were two major events in the phylogenetic history of nematode *selt*. At the root of *Chromadorea* (after the split with *Enoplea*), the Sec codon in *selt* was converted to a Cys codon, concomitant with the loss of the SECIS element. Later in *Rhabditoidea*, likely after the split of *C. japonica*, a *selt* gene duplication occurred resulting in the two extant genes, *selt-1.1* and *selt-1.2*. The reconstructed phylogenetic tree of *selt* genes (Fig. 2) is consistent with this history. An additional feature of nematodes SELT is the presence of a short N-terminal insertion rich in charged and hydroxylated amino acid residues (**Supplementary Fig. 1**), suggesting lineage specific interactions or post-translational modifications.

Finally, we performed thorough searches of other members of the redoxin family (SELENOV, SELENOW, SELENOH and Rdx12) in *C. elegans* and nematode genomes. SELENOT is the single member of this protein family present in nematodes. This makes the model organism *C. elegans* a valuable tool to study SELENOT function.

3.2. SELT-1.1 is expressed in neurons, epithelial and muscle cells

We first examined the expression of *selt-1.1* during the life cycle of *C. elegans*. In hermaphrodites and males GFP expression was observed in neurons, epithelial and muscle cells of transgenic animals carrying both transcriptional (i.e. *selt-1.1* promoter driving GFP expression) and translational (i.e. containing *selt-1.1* promoter, exons and introns driving GFP expression) constructs (Fig. 3). Since *selt-1.1* seemed to be broadly expressed in the nervous system, we crossed two integrated *Pselt-1.1::selt-1.1::gfp* strains with a strain expressing the pan-neuronal marker *rab-3* fused to the red fluorescent protein (RFP) in the nuclei [34]. These crosses confirmed that SELT-1.1 is expressed in all neurons of the nervous system (Fig. 3**A and C**). The expression of *selt-1.1* in the ADL, ASH, ASI, ASJ, ASK, AWB amphid sensilla neurons was also confirmed by DiI staining (**Supplementary Fig. 3**) [35,36]. In the epithelia, *selt-1.1* is expressed in the hypodermal, arcade, pharyngeal, vulval and rectal cells (Fig. 3**B and D**). In contrast, *selt-1.1* was not found to be expressed in the intestine or in the gonad. Muscle cells expressing *selt-1.1* include the somatic muscle cells from head, neck and body wall as well as the non-striated pharyngeal muscles (Fig. 3**B and E**). The translational *Pselt-1.1::selt-1.1::gfp* reporter revealed perinuclear localization (Fig. 3), consistent with the ER localization previously reported for mammalian SELENOT [12]. The ER localization of SELT-1.1 was confirmed by expressing into the QW1266*[Pselt-1.1::selt-1.1::gfp]* the ER marker *tram-1* fused to mcherry in muscle cells [37] (Fig. 3**E**). SELT-1.1 expression was observed throughout development, from pre-bean embryonic stages to the adult stage. Embryos expressed GFP in most cells, also with a perinuclear localization (Fig. 4).

3.3. SELT-1.2 is only expressed in AWB neurons

In contrast to *selt-1.1*, both *Pselt-1.2::selt-1.2::gfp* and *Pselt-1.2::gfp* reporters were expressed exclusively in a single pair of bilateral symmetric sensory neurons located in the amphid, the main chemosensory organ of *C. elegans*. The neuron was identified as AWB by axon morphology, cell body position and by the co-localization with DiI dye (Fig. 5**C**). AWB neurons play a role in volatile avoidance to aversive odorants such as 1-octanol and 2-nonanone [36]. Since the promoter sequence of *selt-1.2* comprises only 0.6 kbp (see Fig. 1), we generated a second transcriptional reporter of *selt-1.2* using 2 kbp upstream of its coding sequence. This additional *selt-1.2* reporter was also expressed in AWB neurons, exclusively. Although SELENOT has been reported to be associated to the ER and the hydrophobic region that interrupts the Trx domain is, presumably, responsible for this localization, *Pselt-1.2::selt-1.2::gfp* translational reporter is present in AWB soma, dendrites and axon (Fig. 5**A**). We amplified *selt-1.2* cDNA to examine whether mRNA variants may lead to different SELT-1.2 isoforms targeting the protein to different compartments. However, only the full length coding sequence predicted by the current gene model of the wormbase was amplified. GFP was detected from L1 larval stage to adult worms (in both hermaphrodites and males). Although we could not observed GFP expression in embryos, *selt-1.2* mRNA was detected by RT-PCR in these stages (data not shown).

3.4. *selt-1.1(tm3763)* and *selt-1.2(tm3771)* null mutants are viable, but the *selt-1.1(tm3763)* mutant is compromised under oxidative stress

To determine the function of SELT in *C. elegans* we analyzed the *selt-1.1(tm3763)*, *selt-1.2(tm3771)* and the *selt-1.1(tm3763)*; *selt-1.2(tm3771)* mutant strains. The deletion allele *selt-1.1(tm3763)* lacks a complete Trx domain, including its redox active site. The *selt-1.2(tm3771)* deletion allele lacks an entire Trx hemidomain required for Trx function (Fig. 1). Thus, these mutants are most likely, null mutants. Both *selt-1.1(tm3763)* and *selt-1.2(tm3771)* mutants as well as the *selt-1.1(tm3763)*; *selt-1.2(tm3771)* double mutant strain are viable,

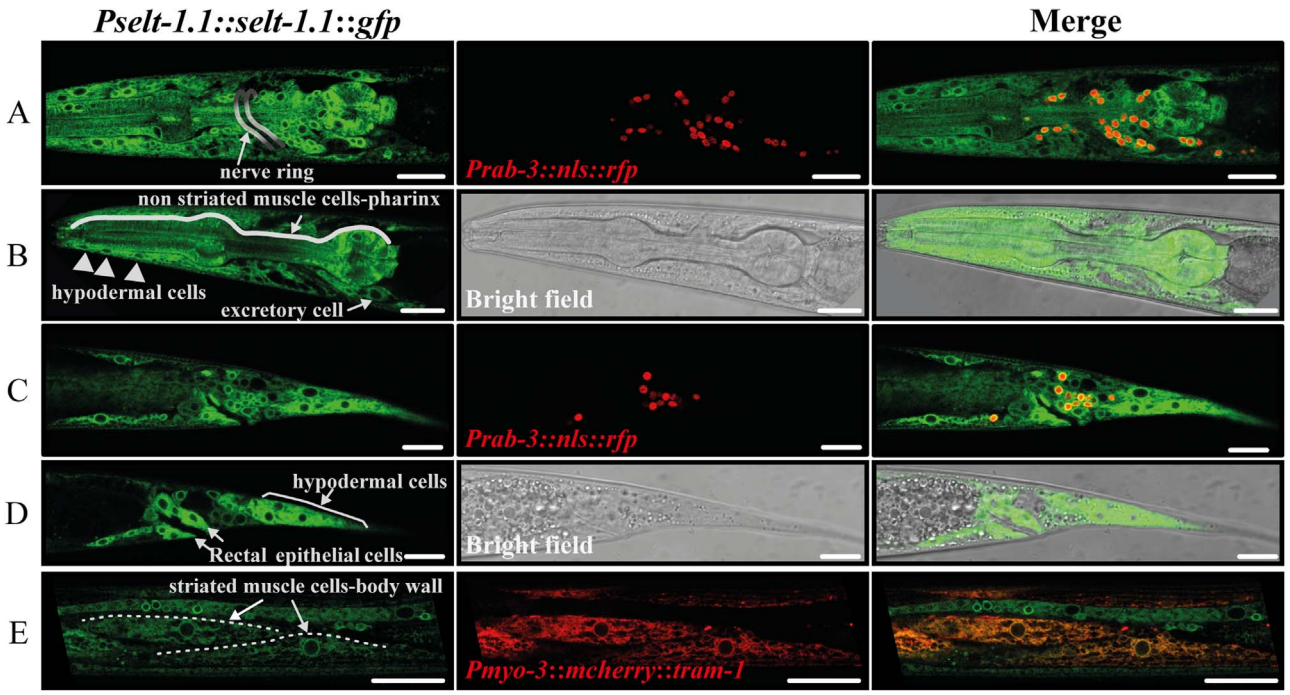

Fig. 3. *selt-1.1* is expressed in neurons, epithelial and muscle cells with an endoplasmic reticulum localization. Confocal images of selected planes at the same magnification show head, tail and mid-body regions. (A) Lateral view of the head of an L4 worm. Transgenic animals simultaneously expressing *Pselt-1.1::selt-1.1::gfp* and *Prab-3::nls::rfp* (neuronal nuclear reporter) show the expression of *selt-1.1* in neurons anterior and posterior to the nerve ring. (B) Head lateral view of an adult worm. Hypodermal cells, pharynx muscle and the excretory cell are indicated. (C) Transgenic animals simultaneously expressing *Pselt-1.1::selt-1.1::gfp* and *Prab-3::nls::rfp* show colocalization in tail neurons. (D) Tail lateral view of an adult worm. Hypodermal cells and rectal epithelium are indicated. (E) Middle body portion of an L4 worm. ER localization of SELT-1.1 fused to GFP. Transgenic animals simultaneously expressing *Pselt-1.1::selt-1.1::gfp* and *Pmyo-3::mcherry::tram-1* (muscle cell ER reporter) show colocalization in the ER of body wall muscle cells, as demonstrated by the yellow color of the merged image. Scale bar: 20 μm. (For interpretation of the references to color in this figure legend, the reader is referred to the web version of this article).

allowing to assess the impact of SELENOT deficiency at an organismal level. *selt-1.1(tm3763)*, *selt-1.2(tm3771)* and the double mutant strain showed normal development, anatomy, motility, lifespan and brood size (Supplementary Fig. 4).

Because SELENOT is a presumed ER oxidoreductase, we interfered the expression of each thiol-disulfide oxidoreductase possessing the ER retention motif KDEL or HDEL (Supplementary Table 2). Neither differences in viability nor obvious phenotype were observed between

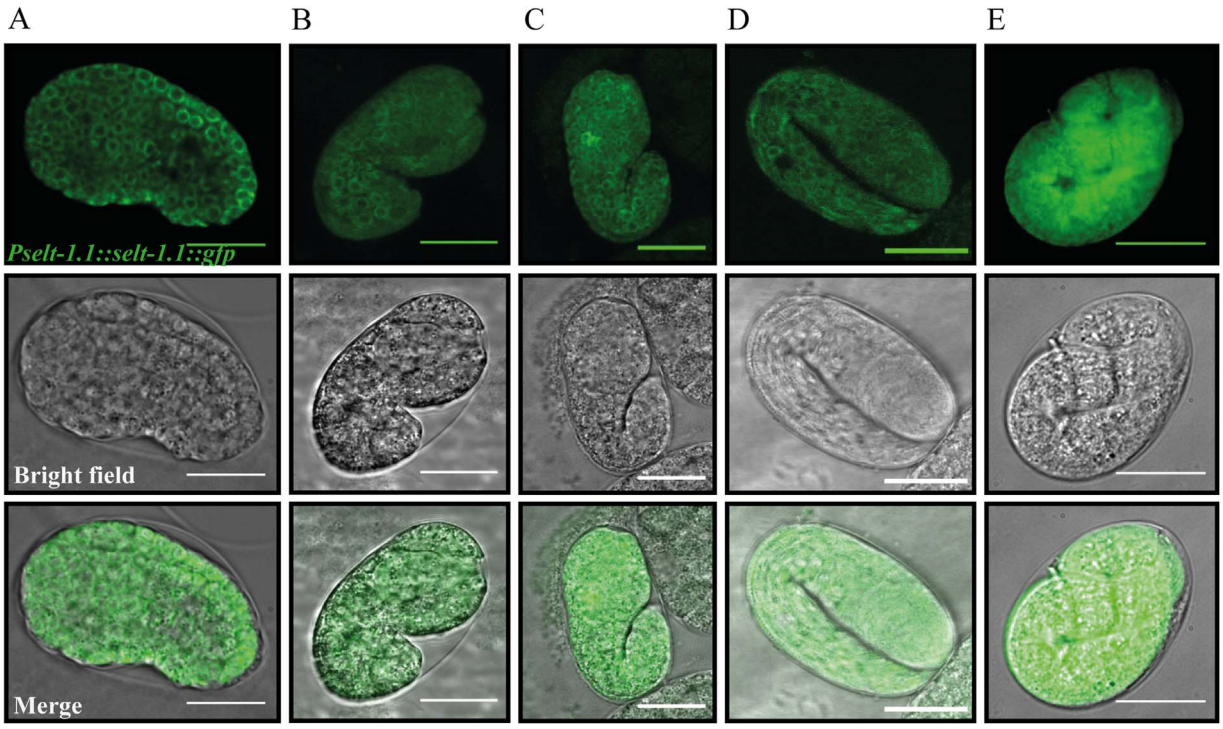

Fig. 4. *selt-1.1* is expressed during embryogenesis from the epidermal enclosure stage. Transgenic animals expressing translational construct *Pselt-1.1::selt-1.1::gfp*, visualized by fluorescence microscopy. The stages shown are: bean (A), comma (B), 1-fold (C), 2-fold (D) and 3-fold (E) stage. Scale bar 20 μm.

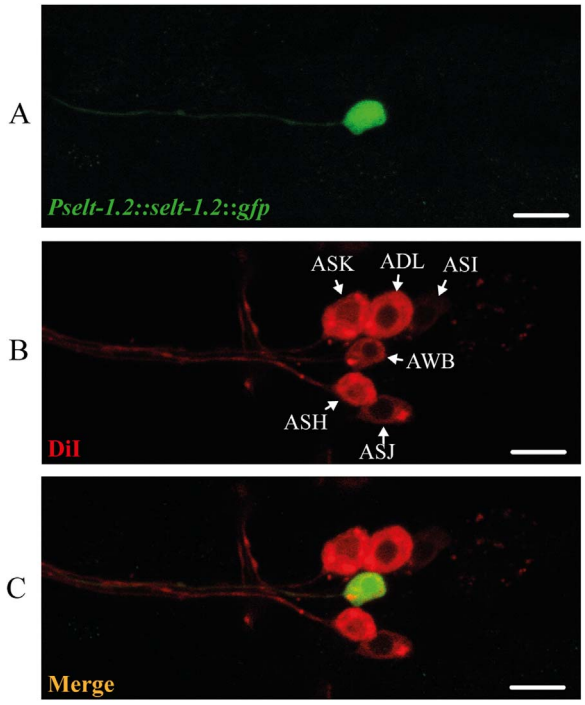

Fig. 5. *selt-1.2* is expressed in AWB neurons. Lateral view. (A) Expression of the translational construct *Pselt-1.2::selt-1.2::gfp* in AWB. (B) Dye-filling with DiI of transgenic animal expressing *Pselt-1.2::selt-1.2::gfp*. (C) Merge. Scale bar 10 μm.

N2 and the double *selt-1.1(tm3763); selt-1.2(tm3771)* mutant strain upon RNAi of the 13 oxidoreductases.

In mammals, rotenone oxidative stress triggers *SELENOT* expression in dopaminergic neurons, and the conditional *SELENOT* KO mice are more susceptible to neurodegenerative rotenone stress [38]. Thus, we stressed the adults ***selt-1.1*** mutant with rotenone 50 μM during 4 h in liquid culture. This strain was more susceptible to rotenone stress than N2. After 60 h of recovery with OP50, 16% of wild-type worms survived, while no *selt-1.1* mutant worm were alive (Fig. 6). Similar results were obtained allowing for one hour worm recovery.

3.5. *2-nonanone aversion is impaired in a selt-1.1 mutant deletion strain*

Since *selt-1.1* is expressed in most neurons and *selt-1.2* is expressed in the AWB chemosensory neurons involved in avoidance to aversive chemicals, we examined the avoidance behavior of the mutant strains towards the aversive odorant 2-nonanone. Strikingly, in the *selt-1.1(tm3763)*, but not in the *selt-1.2(tm3771)* mutant, is impaired the aversive response to 2-nonanone (Fig. 7). The double mutant strain showed an avoidance index similar to the *selt-1.1(tm3763)* mutant. Similarly, aversion to 1-octanol was impaired in the *selt-1.1(tm3763)* strain, (**Supplementary Fig. 5**). These results indicate that *selt-1.1*, but not *selt-1.2*, would be involved in 2-nonanone and 1-octanol aversion. Interestingly, *selt-1.1* is expressed in the three pairs of neurons that detect volatile repellants (ASH, ADL, and AWB, **Supplementary Fig. 3**).

A detailed behavioral analysis of *selt-1.1(tm3763)*, *selt-1.2(tm3771)* and the *selt-1.1*(*tm3763*); *selt-1.2(tm3771)* mutant strains showed that chemoattraction to isoamyl alcohol was not affected compared to N2 (**Supplementary Fig. 6**).

3.6. *selt-1.1 is required for Serratia marcescens and Pseudomonas aeruginosa avoidance*

Since *selt-1.1* is involved in 2-nonanone avoidance and it is expressed in most neurons, and *selt-1.2* is expressed in AWB, which is involved in *S. marcescens* avoidance behavior [26], we examined whether SELT plays a role in the avoidance of bacterial pathogens. Both the *selt-1.1(tm3763)* mutant strain and the double mutant strain were unable to exit the bacterial lawn (Fig. 8**A and B**). Importantly, the *Pselt-1.1::selt-1.1::gfp* expression in the *selt-1.1(tm3763)* mutant strain rescued the mutant phenotype (Fig. 8**B**). In contrast, the avoidance behavior to *S. marcescens* of *selt-1.2*(*tm3771*) mutant was similar to that of wild-type (Fig. 8**A and B**). These results indicate that *selt-1.1*, but not *selt-1.2*, is required in *S. marcescens* avoidance.

Since *P. aeruginosa* PA14 is also a pathogenic bacteria for *C. elegans*, we then examined the lawn avoidance behavior of *selt* mutants. Similar to the results obtained with *S. marcescens,* the *selt-1.1(tm3763)* but not the *selt-1.2(tm3771)* mutant, showed impaired avoidance of *P. aeruginosa* (Fig. 8**B**).

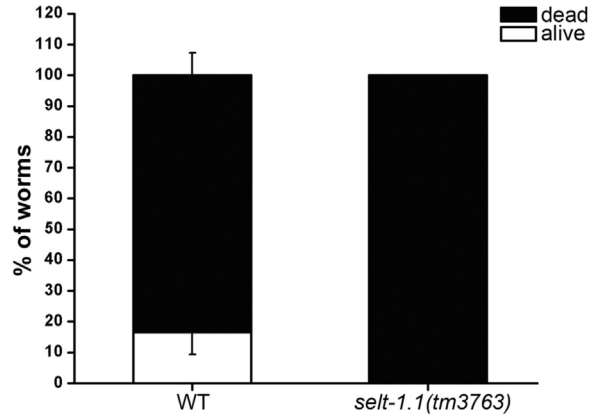

Fig. 6. Rotenone-induced oxidative stress is decreased in *selt-1.1* mutant. N2 and *selt-1.1* mutant were exposed to 50 μM rotenone during 4 h. Columns indicate the percentage of worms alive (white) or dead (black). The graph corresponds to a representative assay with 2 plates per strain, 200 worms/plate. Three biological replicates were performed for this experiment with similar results. Error bars indicate SEM (standard error of the mean).

4. Discussion

The detailed phylogenetic reconstruction of SELENOT in nematodes revealed that Sec is the ancestral amino acid in the nematode lineage, and a Sec→Cys replacement occurred in the *Chromadorea* lineage. This is consistent with the fact that in eukaryotes Cys→Sec substitutions

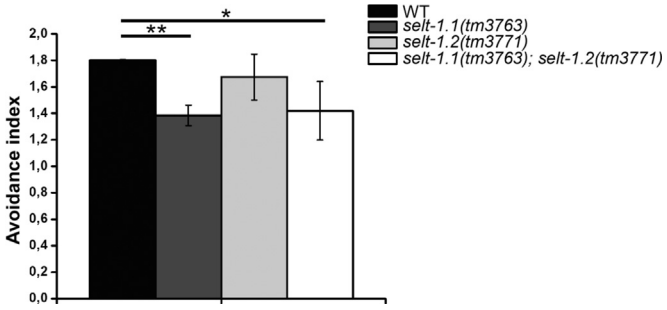

Fig. 7. *selt-1.1* is involved in 2-nonanone avoidance. Columns indicate the avoidance index to 2-nonanone. Wild-type and *selt* mutant strains were subjected to the avoidance assay with 0.6 μL of 2-nonanone. Animals are placed in the center of the plate and observed which sector they enter during 12 min. The scoring method detects either repulsion (higher avoidance index) or attraction (lower index) reflecting an average of avoidance distances of the animals from the center line of the plate. WT, wild-type, *selt-1.1; selt-1.2* correspond to *selt-1.1(tm3763)*; *selt-1.2(tm3763)* double mutant. Asterisks indicate a significant difference from the N2 value: (** $p = 0.0007$; * $p = 0.04$ by unpaired *t*-test). Values are mean ± standard deviation (SD). The graph correspond to an assay with 2 plates per strain, 40–60 worms each. Six biological replicates were performed for this experiment with similar results.

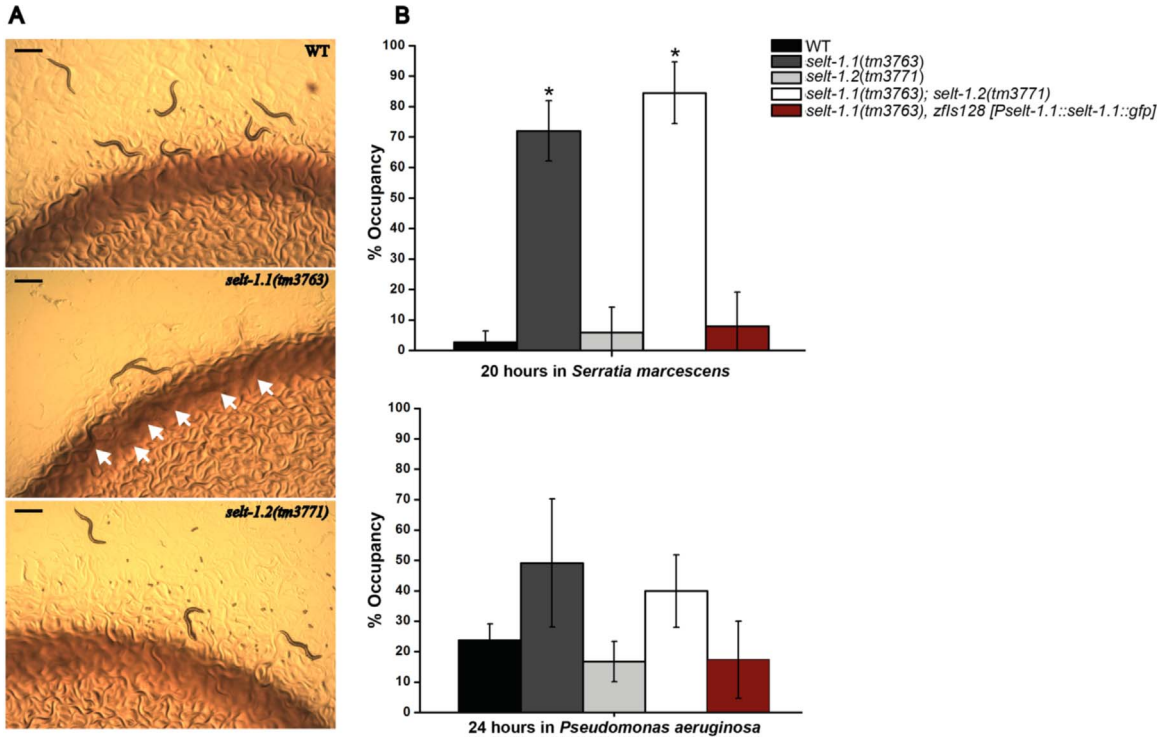

Fig. 8. *selt-1.1* is involved in pathogenic bacteria lawn avoidance behavior. (A) N2, *selt-1.1(tm3763)* and *selt-1.2(tm3771)* strains in *S. marcescens* assay plates are shown. Arrows indicate worms into the bacteria lawn. Scale bars correspond to 500 µm. (B) Lawn occupancy on *S. marcescens* by N2 and *selt* mutants at 20 h and on *P. aeruginosa* at 24 h. Asterisks denote significant differences from the N2 and *selt-1.1(tm3763), zfIs128 [Pselt-1.1::selt-1.1::gfp]* value (*p = 0.02592, ANOVA and Tukey test). Error bars indicate SD. The results correspond to one representative assay with two plates per strain, 20 worms for *S. marcescens* and 30 worms for *P. aeruginosa* assays. Six biological replicates were performed for these experiments with similar results.

have not been documented [6], likely reflecting the need of a point mutation concomitant with the emergence of a SECIS element in the 3´UTR. Subsequently, a gene duplication occurred in the *Caenorhabditis* lineage leading two different SELENOT.

The animal model *C. elegans* offers key advantages to address the function of the redoxin SELENOT as is the only member of the redoxin family present in this organism and both SELT-1.1 and SELT-1.2 are putative Cys-containing oxidoreductases. Importantly, in contrasts with *SELENOT* deficiency in mice, which leads to early embryonic lethality [13]; our results demonstrate that *selt-1.1(tm3763), selt-1.2(tm3771)* and the double *selt-1.1(tm3763); selt-1.2(tm3771) C. elegans* strains are viable. Thus, *C. elegans* is the first animal in which it is possible to perform studies on SELENOT deficiency throughout its development and lifecycle at the organismal level.

In mice and rats SELENOT has been associated with protection of dopaminergic neurons against oxidative stress and neuroendocrine function [12,13]. A conditional knockout mouse line in which *SELENOT* gene is disrupted in nerve cells exhibited reduced volume of the hippocampus, cerebellum, and cerebral cortex, accompanied by an increase of intracellular reactive oxygen species, indicating that SELENOT exerts a neuroprotective role essential during brain development [39]. Deep sequencing of human transcriptome showed that the brain and the adrenal and pituitary glands are the preferential tissues where SELENOT is expressed (http://www.gtexportal.org/home/gene/SELT [40]). Our results showed that *C. elegans selt-1.1* is expressed early in the embryonic development, from the pre-bean stage, and afterwards throughout the entire life cycle. In the adult worm *selt-1.1* is expressed in all neurons. In sharp contrast, we found that *selt-1.2* expression was restricted to a single pair of neurons (AWB).

The *selt-1.1* mutant provided clues regarding functions that are affected by this gene. We found that this mutant has impaired odorant aversion response to 2-nonanone and 1-octanol. However, the *selt-1.1(tm3763)* mutant strain could not be rescued to the wild-type phenotype by our transgene *zfIs128[Pselt-1.1::selt-1.1::gfp]* (data not shown), suggesting that for this specific phenotype, the wild-type level of expression was not reached. The aversive response to 2-nonanone involves mainly AWB neurons, while aversion to 1-octanol involves AWB, ASH and ADL neurons [41,42]. In both cases the aversion behavior also involves interneurons and muscle cells. Thus, aversion to these volatiles is in agreement with the expression pattern for this gene. It is important to mention that chemoattraction to isoamyl alcohol, a volatile chemical, was not affected in the *selt-1.1* mutant strain showing specificity in the nociceptive responses. Surprisingly, SELT-1.2, which is also expressed in AWB, is not involved in odorant aversion to 2-nonanone under the conditions assayed.

Both *selt-1.1* and *selt-1.2* are expressed in AWB, a pair of neurons involved in avoidance of the nematode pathogenic bacteria *S. marcescens* [26]. We found that *selt-1.1* mutant, but not *selt-1.2*, have a marked decreased in lawn avoidance behavior to *S. marcescens*. This decreased was statistically supported. Furthermore, complementation experiments rescue, to a great extent, this phenotype. Avoidance of *S. marcescens* is associated to the detection of serrawettin W2, a cyclic lipodepsipentapeptide surfactant produced by the bacteria. The detection of this molecule and *S. marcescens* appears to be complex and context-dependent, involving both chemical and mechanosensation and likely involves G protein-coupled chemoreceptors and the Toll-like receptor gene *tol-1* [26,43]. Numerous cues result in initial attraction to *S. marcescens* followed by pathogen avoidance, reflecting an evolutionary balance between attraction to nutrition and pathogen infection. A recent study has implicated CO_2-activated BAG chemosensory neurons as required for avoidance of *S. marscecens* [44]. This study also identified TOL-1 signaling pathway having an important role in

pathogen avoidance. Importantly, the avoidance to *P. aeruginosa* PA14 was also impaired in the *selt-1.1* mutant organism. Besides the impaired avoidance behavior, we observed that the *selt-1.1* mutant worms remain at the edge of the pathogenic bacteria lawn as a bordering-like phenotype (Fig. 8**A**). OLL is another pair of neuron that has been involved in lawn avoidance to bacterial pathogens. HECW-1 activity is required in the OLL sensory neuron pair to negatively regulate pathogen avoidance behavior through inhibition of the neuropeptide receptor NPR-1. Interestingly, *npr-1* mutants showed impaired lawn avoidance and a bordering behavior phenotype [27]. The fact that AWB is involved in 2-nonanone and 1-octanol aversion and in bacterial pathogen avoidance suggests that SELT-1.1 might play a key role in this particular class of neurons.

Our results show that *selt-1.1* mutant worms are more susceptible to rotenone-induced oxidative stress, in agreement with SELENOT protective role of dopaminergic neurons against rotenone treatment in mammals. Rotenone exposure in *C. elegans* activates the p38 MAPK pathway, leading to decreased neurodegeneration of dopaminergic neurons [38]. Interestingly, this pathway is also involved in BAG-dependent detection of CO_2, which promotes pathogen avoidance [44], suggesting that SELT-1.1 could be a component of p38 MAPK pathway.

Overexpression of SELENOT in the catecholaminergic cell line PC12 resulted in an increase of the intracellular Ca^{2+} levels, whereas knockdown of *SELENOT* inhibited PACAP-stimulated release of Ca^{2+} from the ER and reduced growth hormone secretion. *C. elegans* SELT-1.1 has an ER localization, suggesting that SELT-1.1 would be an ER regulator, presumably by a redox-dependent mechanism, that plays an important role in signal transduction.

Surprisingly, we could not detect a phenotype associated to *selt-1.2*. The expression of *selt-1.2* appears to be restricted to the pair of neurons AWB. This suggests that the gene duplication that occurred in the *Caenorhabditis* lineage led to subfunctionalization or neofunctionalization. The *selt-1.2* gene derived from *selt-1.1* by duplication may have specialized into a specific subset of *selt-1.1* functions, or acquire a new specific function yet to be identified. Consistent with this view is the fact that *selt-1.2* showed a cytoplasmic localization.

Our results indicate that SELT-1.1 is required for microbial pathogen avoidance and its deficiency affects the response to nociceptive stimuli, indicating that *selt-1.1* is important for optimal organismal fitness. Our results suggest that SELT-1.1 is a redox ER-signal transducer or transducer regulator that controls important survival behaviors and highlight that *C. elegans* is a valuable model to study SELENOT-dependent processes.

Acknowledgements

We are grateful to the Caenorhabditis Genetics Center (CGC) and the Japanese National Bioresource Project for the Experimental Animal Nematode *C. elegans* for provision of *E. coli* and *C. elegans* strains. This work was supported by FOCEM (MERCOSUR Structural Convergence Fund, [COF 03/11]), International Centre for Genetic Engineering and Biotechnology grant [CRP/URU14-01.ICGEB], NIH grant [GM084491] to M.J.A. and Universidad de la República [CSIC_INI_2013_916]. L.R. was recipient of postgraduate study fellowships from Agencia Nacional de Innovación e Investigación [POS_NAC_2012_1_8660] and Universidad de la República. I.C was recipient of a posdoctoral fellowship from Agencia Nacional de Innovación e Investigación [PD_NAC_2013_11008]. We would like to thank Dr. Marcelo Comini (Institut Pasteur de Montevideo) and Dr. Jennifer Pirri (University of Massachusetts Medical School) for helpful discussions.

Appendix A. Supporting information

Supplementary data associated with this article can be found in the online version at doi:10.1016/j.freeradbiomed.2017.03.021.

References

[1] V.M. Labunskyy, D.L. Hatfield, V.N. Gladyshev, Selenoproteins: molecular pathways and physiological roles, Physiol. Rev. 94 (2014) 739–777, http://dx.doi.org/10.1152/physrev.00039.2013.

[2] U. Schweizer, Selenoproteins in the nervous system development, function and degeneration, in: D.L. Hatfield, M.J. Berry, V.N. Gladyshev (Eds.), Selenium Its Mol. Biol. Role Hum. Heal, 3rd ed, Springer, New York, New York, 2012, pp. 235–248, http://dx.doi.org/10.1007/978-1-4614-1025-6_18.

[3] J. Köhrle, The deiodinase family: selenoenzymes regulating thyroid hormone availability and action, Cell. Mol. Life Sci. 57 (2000) 1853–1863, http://dx.doi.org/10.1007/PL00000667.

[4] J.R. Arthur, R.C. Mckenzie, G.J. Beckett, Immunity enhanced by trace elements: selenium in the immune system, J. Nutr. 133 (2003) 1457–1459.

[5] V.N. Turanov, A. Anton, Malinouski, Mikalai. and Gladyshev, Selenium and Male Reproduction, in: D.L. Hatfield, M.J. Berry, V.N. Gladyshev (Eds.), Selenium Its Mol. Biol. Role Hum. Heal, 3rd ed., Springer, New York, New York, 2012, pp. 409–417, http://dx.doi.org/10.1007/978-1-4614-1025-6_32.

[6] A.V. Lobanov, D.L. Hatfield, V.N. Gladyshev, Eukaryotic selenoproteins and selenoproteomes, Biochim. Biophys. Acta - Gen. Subj. 1790 (2009). http://dx.doi.org/10.1016/j.bbagen.2009.05.014.

[7] V.N. Gladyshev, Selenoproteins and selenoproteomes, in: D.L. Hatfield, M.J. Berry, V.N. Gladyshev (Eds.), Selenium Its Mol. Biol. Role Hum. Heal, 3rd ed., Springer, New York, New York, 2012, pp. 109–123, http://dx.doi.org/10.1007/978-1-4614-1025-6_9.

[8] R.J. Hondal, E.L. Ruggles, Differing views of the role of selenium in thioredoxin reductase, Amino Acids 41 (2011) 73–89, http://dx.doi.org/10.1007/s00726-010-0494-6.

[9] D.L. Hatfield, V.N. Gladyshev, MINIREVIEW how selenium Has altered our understanding of the genetic code, Society 22 (2002) 3565–3576, http://dx.doi.org/10.1128/MCB.22.11.3565.

[10] G.V. Kryukov, V.M. Kryukov, V.N. Gladyshev, New mammalian selenocysteine-containing proteins identified with an algorithm that searches for selenocysteine insertion sequence elements, J. Biol. Chem. 274 (1999) 33888–33897, http://dx.doi.org/10.1074/jbc.274.48.33888.

[11] A. Dikiy, S.V. Novoselov, D.E. Fomenko, A. Sengupta, B.A. Carlson, R.L. Cerny, K. Ginalski, N.V. Grishin, D.L. Hatfield, V.N. Gladyshev, SelT, SelW, SelH, and Rdx 12: genomics and molecular insights into the functions of selenoproteins of a novel thioredoxin-like family, Biochemistry 46 (2007) 6871–6882, http://dx.doi.org/10.1021/bi602462q.

[12] L. Grumolato, H. Ghzili, M. Montero-Hadjadje, S. Gasman, J. Lesage, Y. Tanguy, L. Galas, D. Ait-Ali, J. Leprince, N.C. Guérineau, A.G. Elkahloun, A. Fournier, D. Vieau, H. Vaudry, Y. Anouar, Selenoprotein T is a PACAP-regulated gene involved in intracellular Ca2+ mobilization and neuroendocrine secretion, FASEB J. 22 (2008) 1756–1768, http://dx.doi.org/10.1096/fj.06-075820.

[13] L. Boukhzar, A. Hamieh, D. Cartier, Y. Tanguy, I. Alsharif, M. Castex, A. Arabo, S. El Hajji, J.-J. Bonnet, M. Errami, A. Falluel-Morel, A. Chagraoui, I. Lihrmann, Y. Anouar, Selenoprotein T exerts an essential oxidoreductase activity That protects dopaminergic neurons in mouse models of Parkinson's disease, Antioxid. Redox Signal. 24 (2016) 557–574, http://dx.doi.org/10.1089/ars.2015.6478.

[14] G. Prevost, A. Arabo, L. Jian, E. Quelennec, D. Cartier, S. Hassan, A. Falluel-Morel, Y. Tanguy, S. Gargani, I. Lihrmann, J. Kerr-Conte, H. Lefebvre, F. Pattou, Y. Anouar, The PACAP-regulated gene selenoprotein T is abundantly expressed in mouse and human β-cells and its targeted inactivation impairs glucose tolerance, Endocrinology 154 (2013) 3796–3806, http://dx.doi.org/10.1210/en.2013-1167.

[15] D.L. Sengupta, A., Carlson, B. A., Labunskyy, V. M., Gladyshev, V. N., Hatfield, Selenoprotein T deficiency alters cell adhesion and elevates selenoprotein W expression in murine fibroblast cells., Biochem. Cell Biol. 87 (2009) pp. 953–961. doi:10.1139/o09-064.

[16] S. Castellano, V.N. Gladyshev, R. Guigó, M.J. Berry, SelenoDB 1.0: a database of selenoprotein genes, proteins and SECIS elements, Nucleic Acids Res. 36 (2008) 332–338, http://dx.doi.org/10.1093/nar/gkm731.

[17] D.E. Fomenko, W. Xing, B.M. Adair, D.J. Thomas, V.N. Gladyshev, High-throughput identification of catalytic redox-active cysteine residues, Science 315 (80-) (2007) 387–389, http://dx.doi.org/10.1126/science.1133114.

[18] M. Mariotti, D. Santesmasses, S. Capella-Gutierrez, A. Mateo, C. Arnan, R. Johnson, S. D'Aniello, S.H. Yim, V.N. Gladyshev, F. Serras, M. Corominas, T. Gabaldón, R. Guigó, Evolution of selenophosphate synthetases: emergence and relocation of function through independent duplications and recurrent subfunctionalization, Genome Res. 25 (2015) 1256–1267, http://dx.doi.org/10.1101/gr.190538.115.

[19] S. Brenner, The genetics of Caenorhabditis elegans, Genetics 77 (1974) 71–94, http://dx.doi.org/10.1002/cbic.200300625.

[20] C.C. Mello, J.M. Kramer, D. Stinchcomb, V. Ambros, Efficient gene transfer in C.elegans: extrachromosomal maintenance and integration of transforming sequences, EMBO J. 10 (1991) 3959–3970, http://dx.doi.org/10.1016/0168-9525(92)90342-2.

[21] J. Schindelin, I. Arganda-Carreras, E. Frise, V. Kaynig, M. Longair, T. Pietzsch, S. Preibisch, C. Rueden, S. Saalfeld, B. Schmid, J.-Y. Tinevez, D.J. White, V. Hartenstein, K. Eliceiri, P. Tomancak, A. Cardona, Fiji: an open-source platform for biological-image analysis, Nat. Methods 9 (2012) 676–682, http://dx.doi.org/10.1038/nmeth.2019.

[22] A.D. Edelstein, M.A. Tsuchida, N. Amodaj, H. Pinkard, R.D. Vale, N. Stuurman, Advanced methods of microscope control using μ manager software, J. Biol. Methods 1 (2014) 1–10, http://dx.doi.org/10.14440/jbm.2014.36.

[23] D.E. Fomenko, V.N. Gladyshev, Comparative genomics of thiol oxidoreductases

reveals widespread and essential functions of thiol-based redox control of cellular processes, Antioxid. Redox Signal. 16 (2012) 193–201, http://dx.doi.org/10.1089/ars.2011.3980.
[24] K.D. Kimura, K. Fujita, I. Katsura, Enhancement of odor avoidance regulated by dopamine signaling in Caenorhabditis elegans, J. Neurosci. 30 (2010) 16365–16375, http://dx.doi.org/10.1523/JNEUROSCI.6023-09.2010.
[25] S. Ward, Chemotaxis by the nematode Caenorhabditis elegans: identification of attractants and analysis of the response by use of mutants., in: Proceedings of the Natl. Acad. Sci. U.S.A. 70 pp. 817–821. doi:10.1073/pnas.70.3.817, 1973.
[26] E. Pradel, Y. Zhang, N. Pujol, T. Matsuyama, C.I. Bargmann, J.J. Ewbank, Detection and avoidance of a natural product from the pathogenic bacterium Serratia marcescens by Caenorhabditis elegans., in: Proceedings of the Natl. Acad. Sci. U.S.A. 104 pp. 2295–2300. doi:10.1073/pnas.0610281104, 2007.
[27] H.C. Chang, J. Paek, D.H. Kim, Natural polymorphisms in C. elegans HECW-1 E3 ligase affect pathogen avoidance behaviour, Nature 480 (2011) 525–529, http://dx.doi.org/10.1038/nature10643.
[28] M. Mariotti, R. Guigó, Selenoprofiles: profile-based scanning of eukaryotic genome sequences for selenoprotein genes, Bioinformatics 26 (2010) 2656–2663, http://dx.doi.org/10.1093/bioinformatics/btq516.
[29] S. Guindon, J.F. Dufayard, V. Lefort, M. Anisimova, W. Hordijk, O. Gascuel, New algorithms and methods to estimate maximum-likelihood phylogenies: Assessing the performance of PhyML 3.0, Syst. Biol. 59 (2010) 307–321, http://dx.doi.org/10.1093/sysbio/syq010.
[30] M. Mariotti, P.G. Ridge, Y. Zhang, A.V. Lobanov, T.H. Pringle, R. Guigo, D.L. Hatfield, V.N. Gladyshev, Composition and evolution of the vertebrate and mammalian selenoproteomes, PLoS One 7 (2012). http://dx.doi.org/10.1371/journal.pone.0033066.
[31] E.W. Sayers, T. Barrett, D.A. Benson, S.H. Bryant, K. Canese, V. Chetvernin, D.M. Church, M. Dicuccio, R. Edgar, S. Federhen, M. Feolo, L.Y. Geer, W. Helmberg, Y. Kapustin, D. Landsman, D.J. Lipman, T.L. Madden, D.R. Maglott, V. Miller, I. Mizrachi, J. Ostell, K.D. Pruitt, G.D. Schuler, E. Sequeira, S.T. Sherry, M. Shumway, K. Sirotkin, A. Souvorov, G. Starchenko, T.A. Tatusova, L. Wagner, E. Yaschenko, J. Ye, Database resources of the National Center for Biotechnology Information, Nucleic Acids Res. 37 (2009) 5–15, http://dx.doi.org/10.1093/nar/gkn741.
[32] K. Kiontke, N.P. Gavin, Y. Raynes, C. Roehrig, F. Piano, D.H.a. Fitch, Caenorhabditis phylogeny predicts convergence of hermaphroditism and extensive intron loss., in: Proceedings of the Natl. Acad. Sci. U.S.A. 101 pp. 9003–9008. doi:10.1073/pnas.0403094101, 2004.
[33] B.H.M. Meldal, N.J. Debenham, P. De Ley, I.T. De Ley, J.R. Vanfleteren, A.R. Vierstraete, W. Bert, G. Borgonie, T. Moens, P.A. Tyler, M.C. Austen, M.L. Blaxter, A.D. Rogers, P.J.D. Lambshead, An improved molecular phylogeny of the Nematoda with special emphasis on marine taxa, Mol. Phylogenet. Evol. 42 (2007) 622–636, http://dx.doi.org/10.1016/j.ympev.2006.08.025.
[34] N. Stefanakis, I. Carrera, O. Hobert, Regulatory logic of pan-neuronal gene expression in C. elegans, Neuron 87 (2015) 733–750, http://dx.doi.org/10.1016/j.neuron.2015.07.031.
[35] P.N. Inglis, G. Ou, M.R. Leroux, J.M. Scholey, The sensory cilia of Caenorhabditis elegans, WormBook (2007) 1–22, http://dx.doi.org/10.1895/wormbook.1.126.2.
[36] C.I. Bargmann, Chemosensation in C. elegans, WormBook (2006) 1–29, http://dx.doi.org/10.1895/wormbook.1.123.1.
[37] F. Muñoz-Lobato, M.J. Rodríguez-Palero, F.J. Naranjo-Galindo, F. Shephard, C.J. Gaffney, N.J. Szewczyk, S. Hamamichi, K.A. Caldwell, G.A. Caldwell, C.D. Link, A. Miranda-Vizuete, Protective role of DNJ-27/ERdj5 in Caenorhabditis elegans models of human neurodegenerative diseases, Antioxid. Redox Signal. 20 (2014) 217–235, http://dx.doi.org/10.1089/ars.2012.5051.
[38] M.R. Chikka, C. Anbalagan, K. Dvorak, K. Dombeck, V. Prahlad, The mitochondria-regulated immune pathway activated in the C. elegans intestine is neuroprotective, Cell Rep. 16 (2016) 2399–2414, http://dx.doi.org/10.1016/j.celrep.2016.07.077.
[39] M.T. Castex, A. Arabo, M. Bénard, V. Roy, V. Le Joncour, G. Prévost, J.-J. Bonnet, Y. Anouar, A. Falluel-Morel, Selenoprotein, T deficiency leads to neurodevelopmental abnormalities and Hyperactive behavior in mice, Mol. Neurobiol. (2015). http://dx.doi.org/10.1007/s12035-015-9505-7.
[40] The Broad Institute of MIT and Harvard, GTEx, (n.d.). 〈http://www.gtexportal.org/home/gene/SELT〉 (accessed 12 October 2016).
[41] E.R. Troemel, B.E. Kimmel, C.I. Bargmann, Reprogramming chemotaxis responses: Sensory neurons define olfactory preferences in C. elegans, Cell 91 (1997) 161–169, http://dx.doi.org/10.1016/S0092-8674(00)80399-2.
[42] M.Y. Chao, H. Komatsu, H.S. Fukuto, H.M. Dionne, A.C. Hart, Feeding status and serotonin rapidly and reversibly modulate a Caenorhabditis elegans chemosensory circuit., in: Proceedings of the Natl. Acad. Sci. U. S. A. 101 15512–15517. doi:10.1073/pnas.0403369101, 2004.
[43] N. Pujol, E.M. Link, L.X. Liu, C.L. Kurz, G. Alloing, M.W. Tan, K.P. Ray, R. Solari, C.D. Johnson, J.J. Ewbank, A reverse genetic analysis of components of the Toll signaling pathway in Caenorhabditis elegans, Curr. Biol. 11 (2001) 809–821, http://dx.doi.org/10.1016/S0960-9822(01)00241-X.
[44] J.P. Brandt, N. Ringstad, Toll-like receptor signaling promotes development and function of sensory neurons required for a C. elegans pathogen-avoidance behavior, Curr. Biol. 25 (2015) 2228–2237, http://dx.doi.org/10.1016/j.cub.2015.07.037.

Supplementary material

Supplementary Fig. 1. Sequences of *selt* from different species. The presumed redox motif (CXXC) is highlighted in dark gray. The redox motif may contain Sec (U) or Cys (C) in homologous position depending on the species. In orange is indicated the Redoxins conserved sequence at the C-terminal end. In light gray is indicated the hydrophobic region which divides the thioredoxin folding unit (indicated by purple lines). The red line indicates the N-terminal insertion present only in *C. elegans* SELT, rich in charged and hydroxylated amino acid residues (indicated in red font).

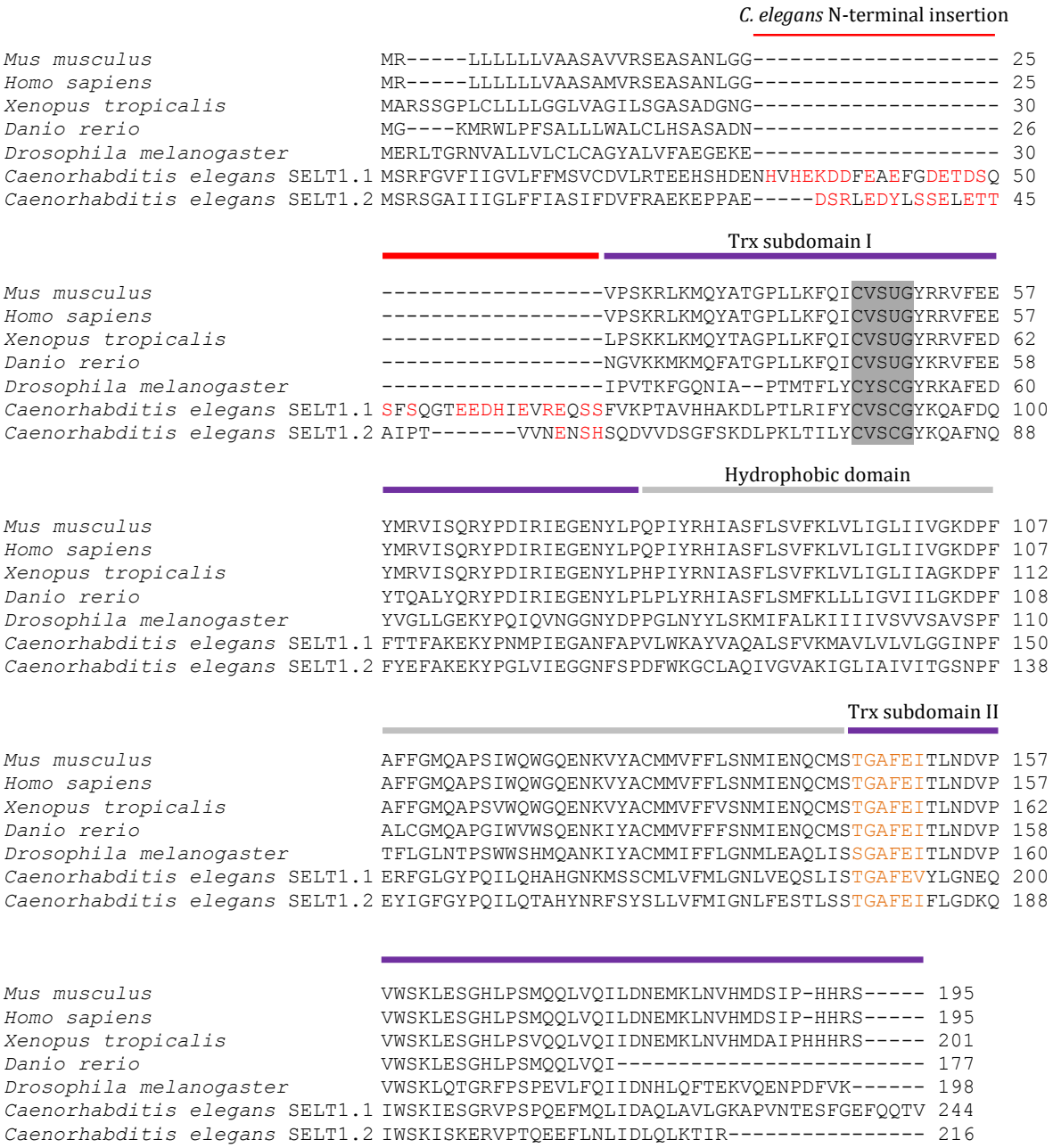

Supplementary Fig. 2. Sec and Cys containing *selt* genes identified across the nematode tree of species. The figure shows a rough phylogenetic tree of nematode species (source: NCBI taxonomy), annotated with the SelT genes that we identified in their genome. SELT proteins containing selenocysteine were found uniquely in the ancestral nematode lineage of Enoplea (bottom). The rest of nematodes (Chromadorea) replaced selenocysteine with cysteine in SELT. Then, a *SELENOT* gene duplication occurred within Rhabditoidea (top).

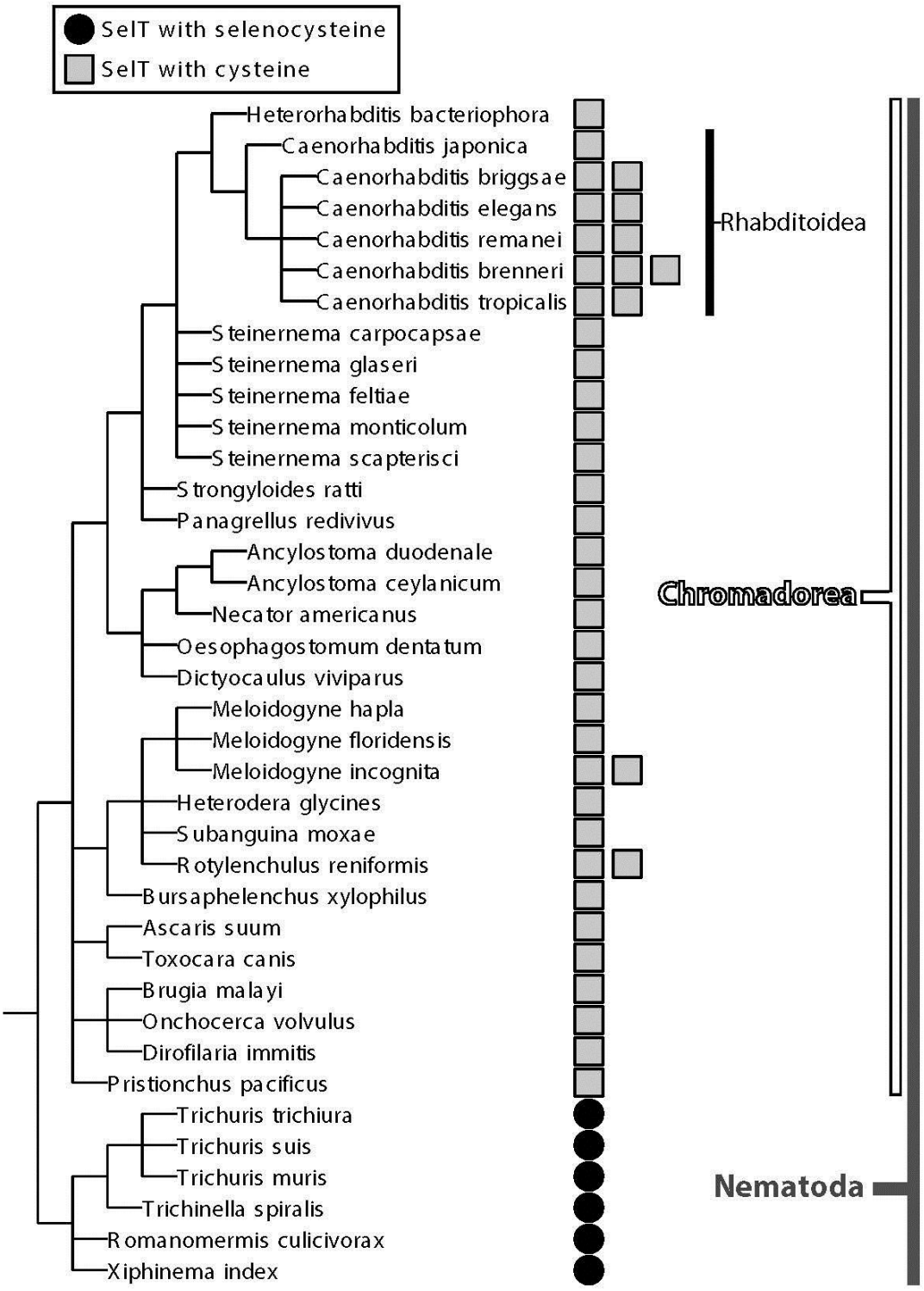

Supplementary Fig. 3. *selt-1.1* is expressed in the chemosensory neurons AWB, ADL and ASH. Confocal images of selected planes at the same magnification show a lateral view of an adult head. (A) Transgenic animals expressing *Pselt-1.1::selt-1.1*::*gfp*. (B) Dye-filling with DiI of transgenic animal expressing *Pselt-1.1::selt-1.1*::*gfp*. (C) Merge. Colocalization in ASI, ASK, ADL, AWB, ASH, ASJ is demonstrated by the yellow color of the merged image. Scale bar: 10 µm.

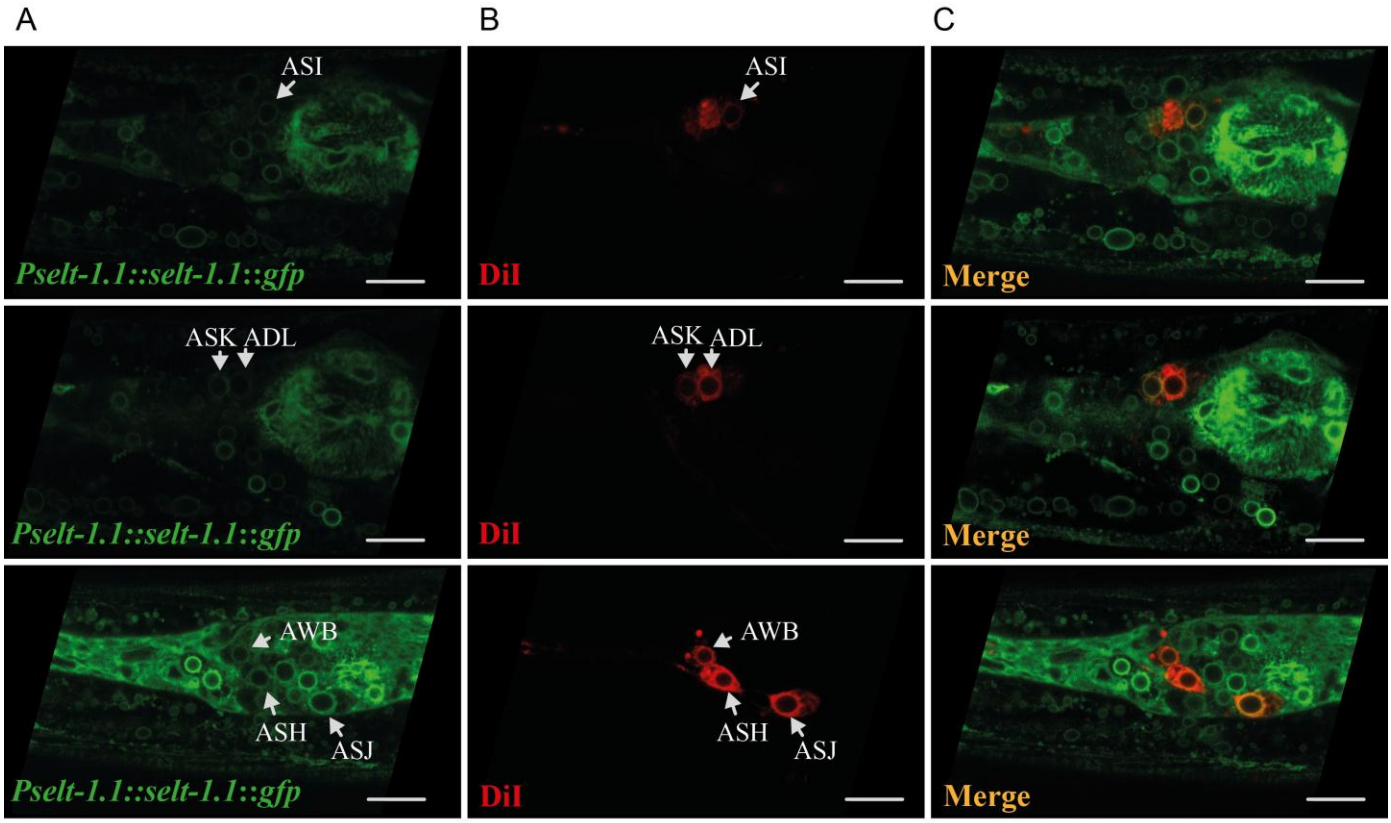

Supplementary Fig. 4. *selt-1.1* mutant strains exhibited normal lifespan and brood size. (A) Columns indicate the brood size of *selt* mutants and wild type (WT) strains. The brood size indicates the number of eggs laid by one animal in its entire life. Each value corresponds to the mean progeny size of 10 worms. The experiment was performed three times, with similar results. Error bars indicate standard deviation (SD). (B) The graph corresponds to the survival curves of *selt* mutants and wild-type strains. The lifespan is measured by the number of days the animal is alive once the adult stage was reached. Each mutant strain was compared with the wild-type strain using the log-rank test (Kaplan-Meier), and no differences were determined.

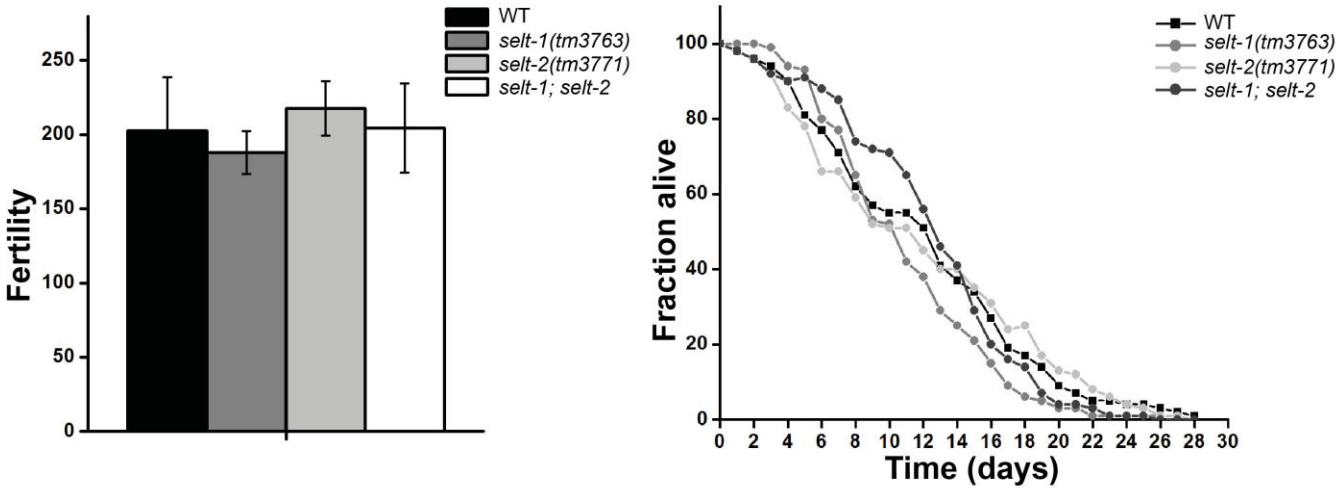

Supplementary Fig. 5. *selt-1.1* is involved in 1-octanol avoidance. Columns indicate the chemotaxis index to 1-octanol. Wild-type and *selt-1.1* mutant strain were subjected to the chemotaxis assay. 1 µL of 1-octanol or control are placed 180 degrees opposite each other close the edges of the plate. Each point includes 1 of sodium azide that will paralyze worms once they reach the destination. Animals are placed in the center of the plate and after 1 hour the number of worms anaesthetized at each point is counted. The chemotaxis index = (number of animals at the odorant – number of animals at control) / total number of animals on the assay plate. WT, N2 wild-type. Asterisk indicates a significant difference from the N2 value: (* p = 0.049 by unpaired *t* test). Values are mean ± standard deviation (SD). The graph corresponds to an assay with 2 plates per strain, 40-60 worms each. Six biological replicates were performed for this experiment with similar results.

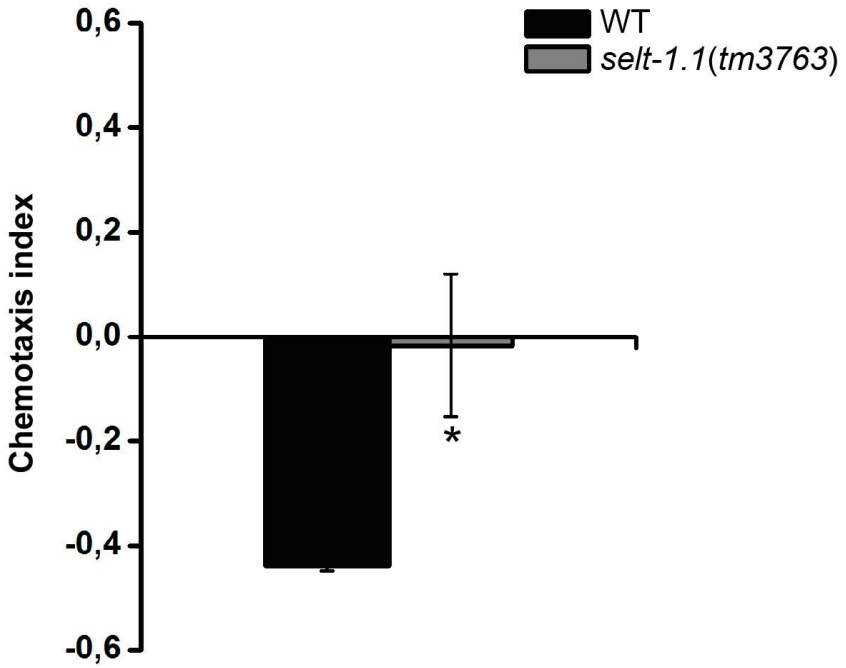

$$CI = \frac{\text{\# worms at 1-octanol - \# worms at control}}{\text{total \# worms}}$$

Supplementary Fig. 6. *selt* mutants show normal chemoattraction to isoamyl alcohol. Columns indicate the chemotaxis index to isoamyl alcohol. Wild-type and *selt* mutant strains were subjected to the chemotaxis assay with 1 µL of isoamyl alcohol (1:100 dilution). Columns indicate the chemotaxis index to 1-octanol. Wild-type and *selt-1* mutant strain were subjected to the chemotaxis assay. 1 µL of 1-octanol or control are placed 180 degrees opposite each other close the edges of the plate. Each point includes 1 of sodium azide that will paralyze worms once they reach the destination. Animals are placed in the center of the plate and after 1 hour the number of worms anaesthetized at each point is counted. The chemotaxis index = (number of animals at the odorant – number of animals at control) / total number of animals on the assay plate. WT, N2 wild-type. Values are mean ± standard deviation (SD). The graph corresponds to an assay with 2 plates per strain, approximately 100 worms each. Three biological replicates were performed for this experiment with similar results.

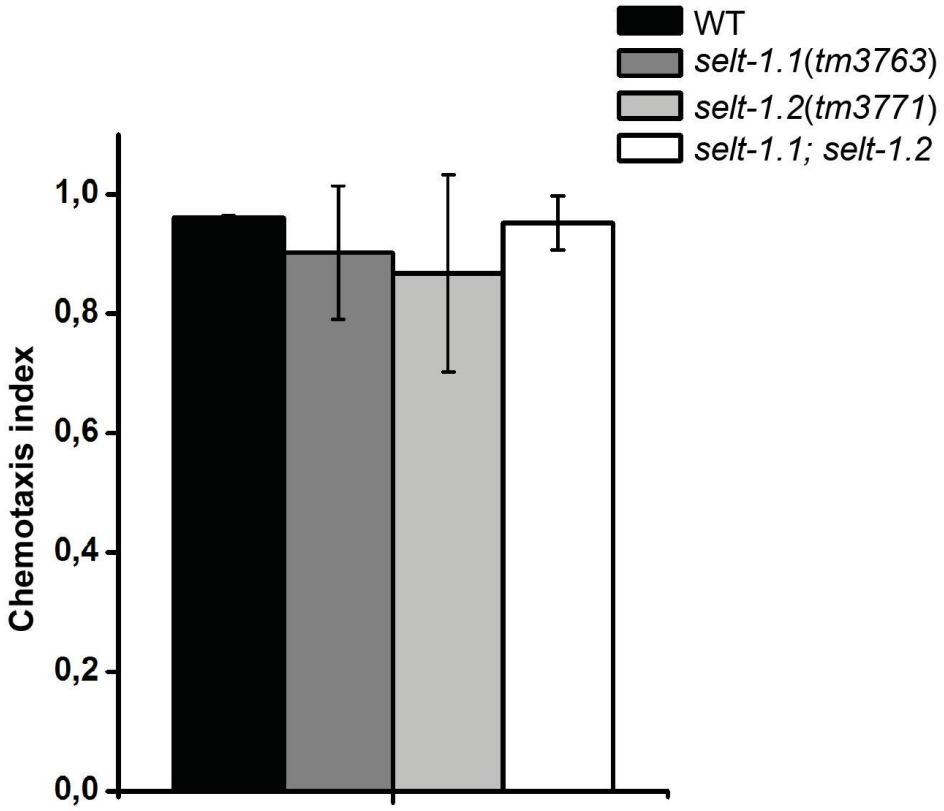

$$CI = \frac{\#\text{ worms at isoamyl alcohol} - \#\text{ worms at control}}{\text{total }\#\text{ worms}}$$

Supplementary Table 1. List of strains used and generated in this study.

Strain	Transgene	Genotype
IH6		*selt-1.1(tm3763) X*
IH7		*selt-1.2(tm3771) V*
IH8		*selt-1.1(tm3763) X; selt-1.2(tm3771)V*
QW1186	*zfex494*	*lin-15(n765ts) X; Ex[Pselt-1.1::gfp, pL15EK]*
QW1187	*zfex495*	*lin-15(n765ts) X; Ex[Pselt-1.2::gfp, pL15EK]*
QW1188	*zfex495*	*lin-15(n765ts) X; Ex[Pselt-1.1::gfp, pL15EK]*
QW1189	*zfex496*	*lin-15(n765ts) X; Ex[Pselt-1.1::gfp, pL15EK]*
QW1213	*zfex522*	*lin-15(n765ts) X; Ex[Pselt-1.1::selt-1.1::gfp, pL15EK]*
QW1214	*zfex523*	*lin-15(n765ts) X; Ex[Pselt-1.1::selt-1.1::gfp, pL15EK]*
QW1215	*zfex524*	*lin-15(n765ts) X; Ex[Pselt-1.1::selt-1.1::gfp, pL15EK]*
QW1216	*zfex525*	*lin-15(n765ts) X; Ex[Pselt-1.1::selt-1.1::gfp, pL15EK]*
QW1265	*zfIs128*	*lin-15(n765ts) X; Pselt-1.1::selt-1.1::gfp, pL15EK V*
QW1266	*zfIs129*	*lin-15(n765ts) X, Pselt-1.1::selt-1.1::gfp, pL15EK X*
QW1244	*zfex541*	*lin-15(n765ts) X; Ex[1.6kb upstream+Pselt-1.2::gfp, pL15EK]*
QW1245	*zfex542*	*lin-15(n765ts) X; Ex[1.6kb upstream+Pselt-1.2::gfp, pL15EK]*
QW1246	*zfex543*	*lin-15(n765ts) X; Ex[1.6kb upstream+Pselt-1.2::gfp, pL15EK]*
QW1248	*zfex545*	*lin-15(n765ts) X; Ex[1.6kb upstream+Pselt-1.2::selt-1.2::gfp, pL15EK]*
QW1249	*zfex546*	*lin-15(n765ts) X; Ex[1.6kb upstream+Pselt-1.2::selt-1.2::gfp, pL15EK]*
QW1247	*zfex544*	*lin-15(n765ts) X; Ex[1.6kb upstream+Pselt-1.2::selt-1.2::gfp, pL15EK]*
QW1257	*zfex551*	*lin-15(n765ts) X; Ex[Pselt-1.2::gfp, pL15EK]*
QW1258	*zfex552*	*lin-15(n765ts) X; Ex[Pselt-1.2::gfp, pL15EK]*
QW1259	*zfex553*	*lin-15(n765ts) X; Ex[Pselt-1.2::gfp, pL15EK]*
QW1260	*zfex554*	*lin-15(n765ts) X; Ex[Pselt-1.2::selt-1.2::gfp, pL15EK]*
IH18	*zfIs129; vzEx91*	*lin-15(n765ts) X, Pselt-1.1::selt-1.1::gfp, pL15EK X; Ex[Pmyo-3::mcherry::tram-1]*
IH19	*zfIs128*	*selt-1.1(tm3763) X; Pselt-1.1::selt-1.1::gfp, pL15EK V*
IH20	*zfIs129; otIs356*	*lin-15(n765ts) X, Pselt-1.1::selt-1.1::gfp, pL15EK X; Prab-3::nls::rfp*
BY250	*vtIs7*	*Pdat-1::dat-1::gfp*
VZ255	*vzEx91*	*Ex[Pmyo-3::mcherry::tram-1]*

Supplementary Table 2. List of genes whose expression was interfered by RNAi.

Gene	Wormbase ID
pdi-1 (C14B1.1)	WBRNAi00010719
pdi-2 (C07A12.4)	WBRNAi00008357
pdi-3 (H06O01.1)	WBRNAi00003873
pdi-6 (B0403.4)	WBRNAi00009753
F49H12.5	WBRNAi00015347
dnj-27 (Y47H9C.5)	WBRNAi00037210
C14B9.2	WBRNAi00010732
Y49E10.4	WBRNAi00020781
nlp-6 (Y73B6BL.12)	WBRNAi00019077
ero-1 (Y105E8B.8)	WBRNAi00036491
C30H7.2	WBRNAi00003044
Y57A10A.23	WBRNAi00021100
C06A6.5	WBRNAi00010264

Supplementary Table 3. List of primers used for cloning.

	Sequence
selt-1.2 transcriptional and translational forward primer	cagaagcttaaccataaaactaattcagtga
selt-1.2 transcriptional reverse primer	acggtcgacttgatagatgaaaagaagtttc
selt-1.2 translational reverse primer	acggtcgacacgaatagttttcaattgaagatc
selt-1.1 transcriptional and translational forward primer	acggtcgacgttagggaatgaaaagttg
selt-1.1 transcriptional reverse primer	acgggatcccccaaaccgtgacatctg
selt-1.1 translational reverse primer	ggatccgacagtctgttggaactctccaaatg